Supporting Information

Silicon phthalocyanines for n-type organic thin-film transistors: development of structure property relationships

*Benjamin King,[1] Owen A. Melville,[1] Nicole A. Rice,[1] Somayeh Kashani,[2] Claire Tonnelé,[4] Hasan Raboui,[5] Sufal Swaraj,[6] Trevor M. Grant,[1] Terry McAfee,[3] Timothy P. Bender,[5,7,8] Harald Ade,[2] Frédéric Castet,[9] Luca Muccioli,[9,10] and Benoît H. Lessard[1,11]**

1. University of Ottawa, Department of Chemical and Biological Engineering, 161 Louis Pasteur, Ottawa, ON, Canada, K1N 6N5
2. Department of Physics and Organic and Carbon Electronics Laboratories (ORaCEL), North Carolina State University, Raleigh, NC, USA
3. Department of Physics and Astronomy, Washington State University, Pullman, WA, USA
4. Donostia International Physics Center, 4 Paseo Manuel de Lardizabal, 20018 Donostia, Euskadi, Spain
5. Department of Chemical Engineering & Applied Chemistry, University of Toronto, 200 College Street, Toronto, Ontario M5S 3E5, Canada
6. Synchrotron SOLEIL, Gif-sur-yvette Cedex, France
7. Department of Materials Science and Engineering, University of Toronto, 180 College Street, Toronto, Ontario M5S 3E5, Canada
8. Department of Chemistry, University of Toronto, 80 St. George Street, Toronto, Ontario M5S 3H6, Canada
9. Université de Bordeaux, Institut des Sciences Moléculaires, 351 Cours de la Libération, 33405 Talence, France
10. University of Bologna, Department of Industrial Chemistry, 4 Viale Risorgimento, 40136 Bologna, Italy
11. School of Electrical Engineering and Computer Science, University of Ottawa, 800 King Edward, Ottawa, ON, Canada K1N 6N5

Table of Contents

Additional Data from DFT Calculations and Single Crystal Data

Table S1. Summary of single-crystal packing motifs, stacking types and π – π stacking distances for materials **1 – 11**. The shortest stacking distance is highlighted in bold.

Material	Bridge	Packing Motif	Stacking Types[a)]	A (Å)	B1 [b)] (Å)	B2 [b)] (Å)	C1 [c)] (Å)	C2 [c)] (Å)	D (Å)	Source
1 (PhO-SiPc)	PhO	Herringbone	2 (AB)	3.771	3.673	**3.564**				[31]
2 (345F-SiPc)	PhO	Herringone	1 (B)		3.716	**3.580**				[30]
3 (F_{10}-SiPc)	PhO	Lamellar	1 (A)	**3.769**						[28]
4 (2MP-SiPc)	PhO	Lamellar	3 (BCD)		**3.567**	3.826	3.862	3.828	3.826	[31]
5 (3MP-SiPc)	PhO	68°	1 (B)		3.797	**3.671**				[31]
6 (4MP-SiPc)	PhO	Lamellar	1 (B)		**3.599**	3.648				[31]
7 (3Pyr-SiPc)	PhO	22°	1 (C)				3.932	**3.709**		[31]
8 (4Pyr-SiPc)	PhO	Herringbone	2 (AB)	3.762	**3.580**	3.601				[31]
9 (3I-SiPc)	PhO	Herringbone	1 (C)				**3.716**	3.810		[33]
10 (PhCOO-SiPc)	R-COO	Lamellar	2 (AB)	3.738	3.882	**3.554**				[19]
11 (NpCOO-SiPc)	R-COO	Lamellar	1 (A)	**3.650**						[19]

a) A = dual benzene-benzene stacking, B = single benzene-benzene and single benzene-isoindole stacking, C = dual benzene-isoindole stacking, D = single benzene-benzene stacking
b) B1 = benzene-isoindole stacking distance, B2 = benzene-benzene stacking distance
c) C1 = benzene-isoindole 1 stacking distance, C2 = benzene-isoindole 2 stacking distance

Table S2. Non-negligible transfer integrals ($J_k \geq 1$, in units of meV), calculated between a reference molecule and its first neighbours. The crystallographic directions corresponding to intermolecular vectors joining the reference molecule with its neighbours are given in the basis of direct lattice vectors.

Material	Direction: J_k
1 (PhO)	±(1, 0, 1): **47**; ±(0, 0, 1): **19**; (0, ±1/2, ±1/2): **7**; ±(1, 0, 0): **1**
2 (345F)	±(1, 0 0): **37**; ±(1/2, ±1/2, 1/2): **10**; ±(1, 0, 1): **14**
3 (F10)	±(1, 0, 0): **43**; ±(1, 0, -1): **12**; ±(0, 1, -1): **5**
4 (2MP)	(0, 1/2, ±1/2): **25**; (-1, 1/2, 1/2): **17**; (0, -1/2, -1/2): **16**; (-1, -1/2, 1/2): **10**; (1, 1/2, -1/2): **10**; (-1, -1/2, -1/2): **2**; ±(1, 0, 0): **1**; ±(0, 1, 0): **1**
5 (3MP)	±(1, 0, 0): **25**; (1/2, ±1/2, 1/2): **11**; (−1/2, ±1/2, −1/2): **10**; ±(1, 0, 1): **8**
6 (4MP)	±(0, 1, 1): **47**; ±(1, -1, 0): **10**; (1, 0, -1): **9**; ±(1, 0, 0): **1**
7 (3Pyr)	±(1, 0, 0): **28**; ±(1, 1/2, 1/2): **6**; ±(1, -1/2, 1/2): **6**; ±(0, 1, 0): **4**
8 (4Pyr)	±(1, 0, 1): **44**; ±(0, 0, 1): **21**; (0, ±1/2, ±1/2): **7**; ±(1, 0, 0): **1**
9 (3I)	±(0, 0, 1): **86**; ±(1, 0, 0): **4**
10 (BnO)	±(0, 0, 1): **34**; ±(1, 0, 0): **20**; ±(1, 1, 1): **10**
11 (NpO)	±(1, 0, 0): **26**; ±(0, 0, 1): **12**; ±(1, 1, 1): **10**; ±(0, 1, 0): **1**

* Compound **10** is not reported since it was not possible to obtain a single crystal

Figure S1. Top views of the molecular dimers giving rise to the largest electronic couplings, as extracted from periodic replicas of experimental crystal structures.

1 (PhO-SiPc)

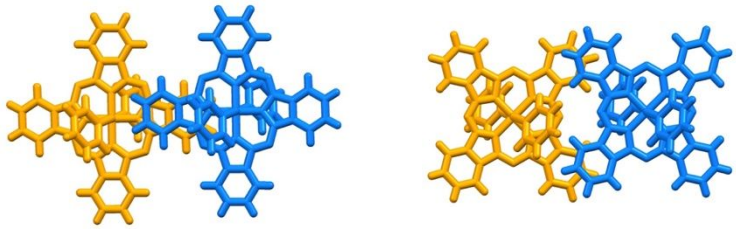

±(1, 0, 1): **47 meV** ±(0, 0, 1): **19 meV**

Figure S1: *continued*.

2 (345F-SiPc)

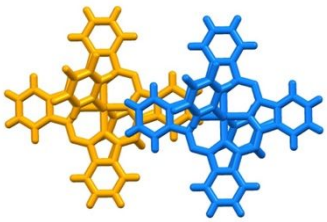

±(1, 0 0): **37 meV**

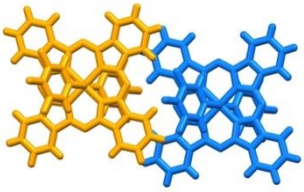

±(1, 0, 1): **14 meV**

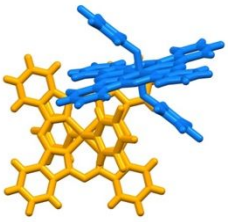

±(1/2, ±1/2, 1/2): **10 meV**

3 (F_{10}-SiPc)

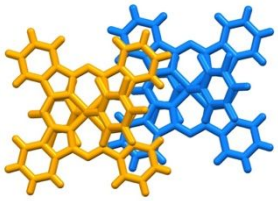

±(1, 0, 0): **43 meV**

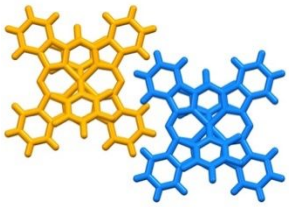

±(1, 0, -1): **12 meV**

4 (2MP-SiPc)

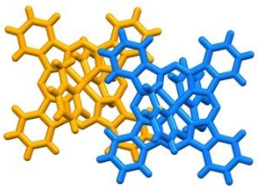

(0, 1/2, -1/2): **25 meV**

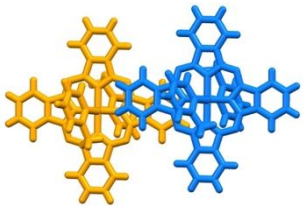

(0, 1/2, 1/2): **25 meV**

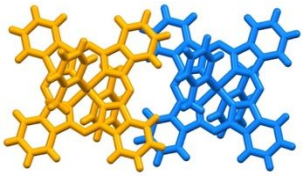

(-1, 1/2, 1/2): **17 meV**

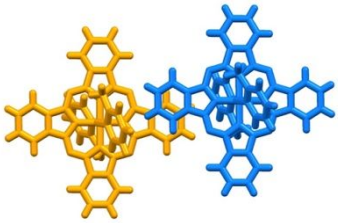

(0, -1/2, -1/2): **16 meV**

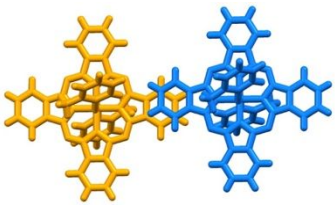

(-1, -1/2, 1/2): **10 meV**

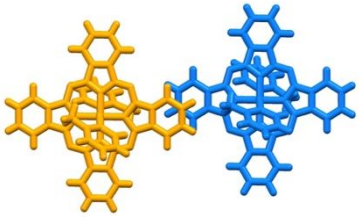

(1, 1/2, -1/2): **12 meV**

Figure S1: *continued*.

5 (3MP-SiPc)

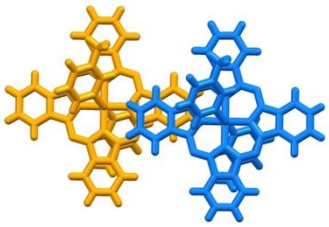

±(1, 0, 0): **25 meV**

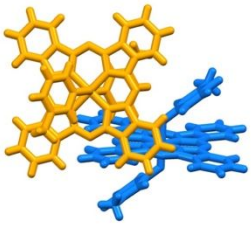

(1/2, ±1/2, 1/2): **11 meV**

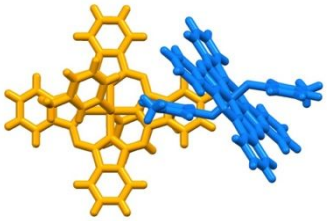

(−1/2, ±1/2, −1/2): **10 meV**

6 (4MP-SiPc)

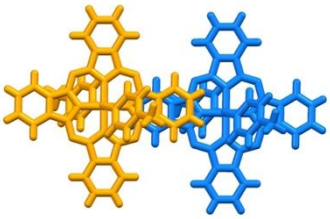

±(0, 1, 1): **47 meV**

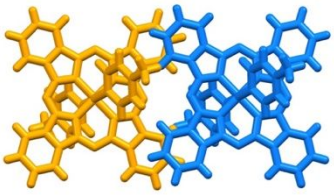

±(1, -1, 0): **10 meV**

7 (3Pyr-SiPc)

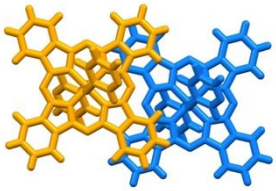

±(1, 0, 0): **28 meV**

8 (4Pyr-SiPc)

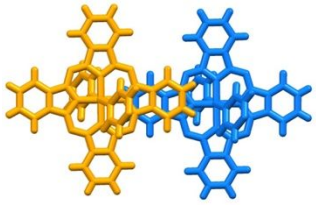

±(1, 0, 1): **44 meV**

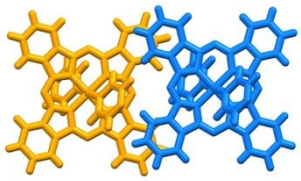

±(0, 0, 1): **21 meV**

Figure S1: *continued*.

9 (3I-SiPc)

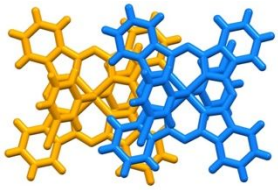

±(0, 0, 1): **86 meV**

10 (PhCOO-SiPc)

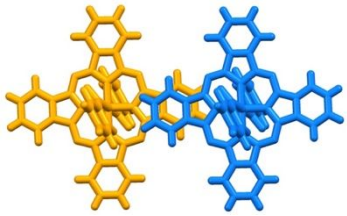

±(0, 0, 1): **34 meV**

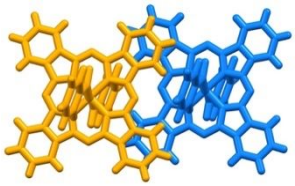

±(1, 0, 0): **20 meV**

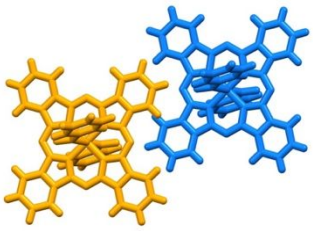

±(1, 1, 1): **10 meV**

11 (NpCOO-SiPc)

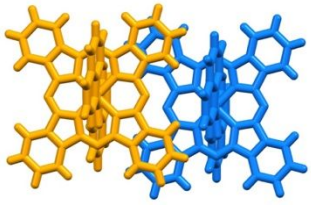

±(1, 0, 0): **26 meV**

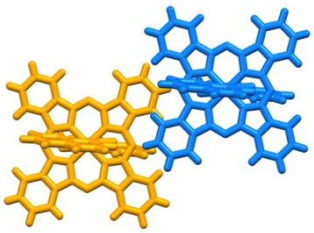

±(0, 0, 1): **12 meV**

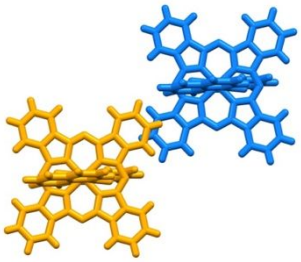

±(1, 1, 1): **10 meV**

Additional Electrical Characterization Data

Table S3. Electrical performance of SiPcs 1 – 11 with Ag electrodes.

Material	μ_e [$cm^2 V^{-1} s^{-1}$][a)]	V_T [V] [a)]	I_{on} [a)]	$I_{on/off}$ [a)]
1 (PhO-SiPc)	7.7 ±7.4 x10^{-3}	40.5 ± 1.8	2.47 x10^{-7}	10^4
2 (345F-SiPc)	4.7±1.1 x10^{-2}	28.9 ± 2.1	6.23 x10^{-6}	10^5
3 (F10-SiPc)	7.1 ± 3.0 x10^{-2}	39.7 ± 1.4	5.68 x10^{-6}	10^5
4 (2MP-SiPc)	1.0 ± 0.30 x10^{-3}	48.7 ± 0.7	3.86 x10^{-8}	10^3
5 (3MP-SiPc)	8.0 ± 1.7 x10^{-3}	34.1 ± 0.4	1.04 x10^{-6}	10^4-10^5
6 (4MP-SiPc)	1.6 ± 0.29 x10^{-2}	41.9 ± 2.1	1.12 x10^{-6}	10^4-10^5
7 (3Pyr-SiPc)	2.0 ± 1.2 x10^{-4}	*	5.90 x10^{-6}	10^0
8 (4Pyr-SiPc)	7.0 ± 2.0 x10^{-3}	*	3.70 x10^{-6}	10^1
9 (3I-SiPc)	4.6 ± 0.74 x10^{-4}	44.5 ± 2.7	2.20 x10^{-8}	10^3
10 (PhCOO-SiPc)	2.3 ± 0.69 x10^{-4}	36.2 ± 7.3	1.90 x10^{-8}	10^2-10^3
11 (NpCOO-SiPc)	3.9 ± 1.5 x10^{-3}	40.7 ± 0.8	2.31 x10^{-7}	10^3-10^4

[a)] μ_e and V_T were calculated based on mean values, while I_{on} and $I_{on/off}$ were calculated based on median values

* Values could not be calculated accurately due to high off current causing deviation from Equation 1

Representative Output and Transfer Curve Data for All SiPc Derivatives

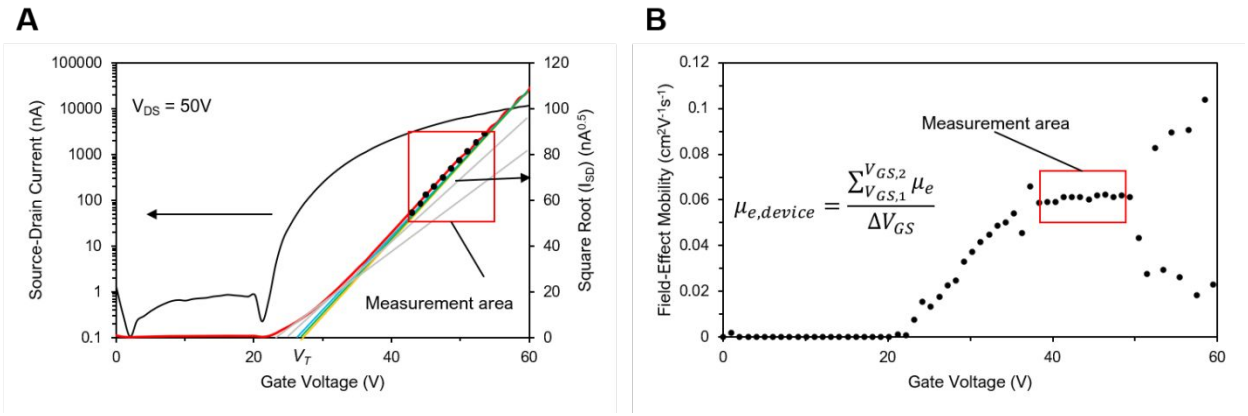

Figure S2. A) Characteristic forward transfer curve and B) μ_e vs V_{GS} for a forward sweep of I_{DS} vs V_{GS} for 345F-SiPc (**2**) with μ_e extracted from the average of values in the measurement area (red box)

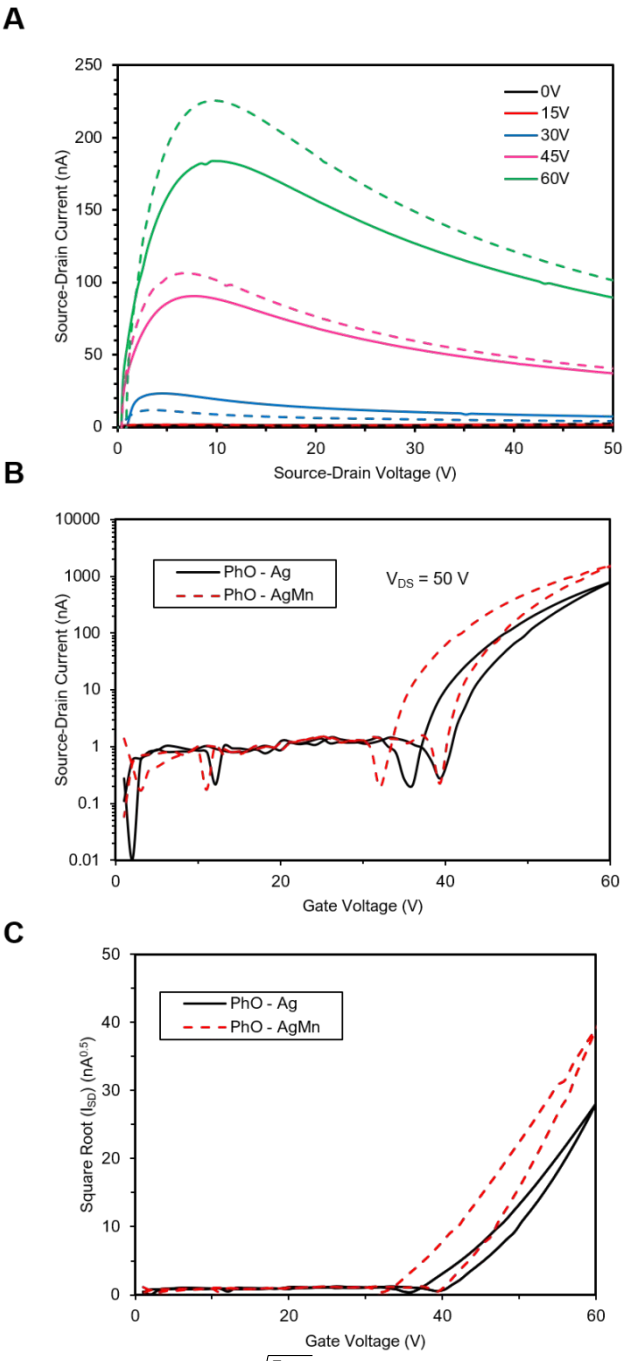

Figure S3: A) Output, B) transfer and C) $\sqrt{I_{DS}}$ vs V_{GS} curves for PhO-SiPc (**1**) with Ag (solid lines) and Ag/Mn (dotted lines) electrode configurations.

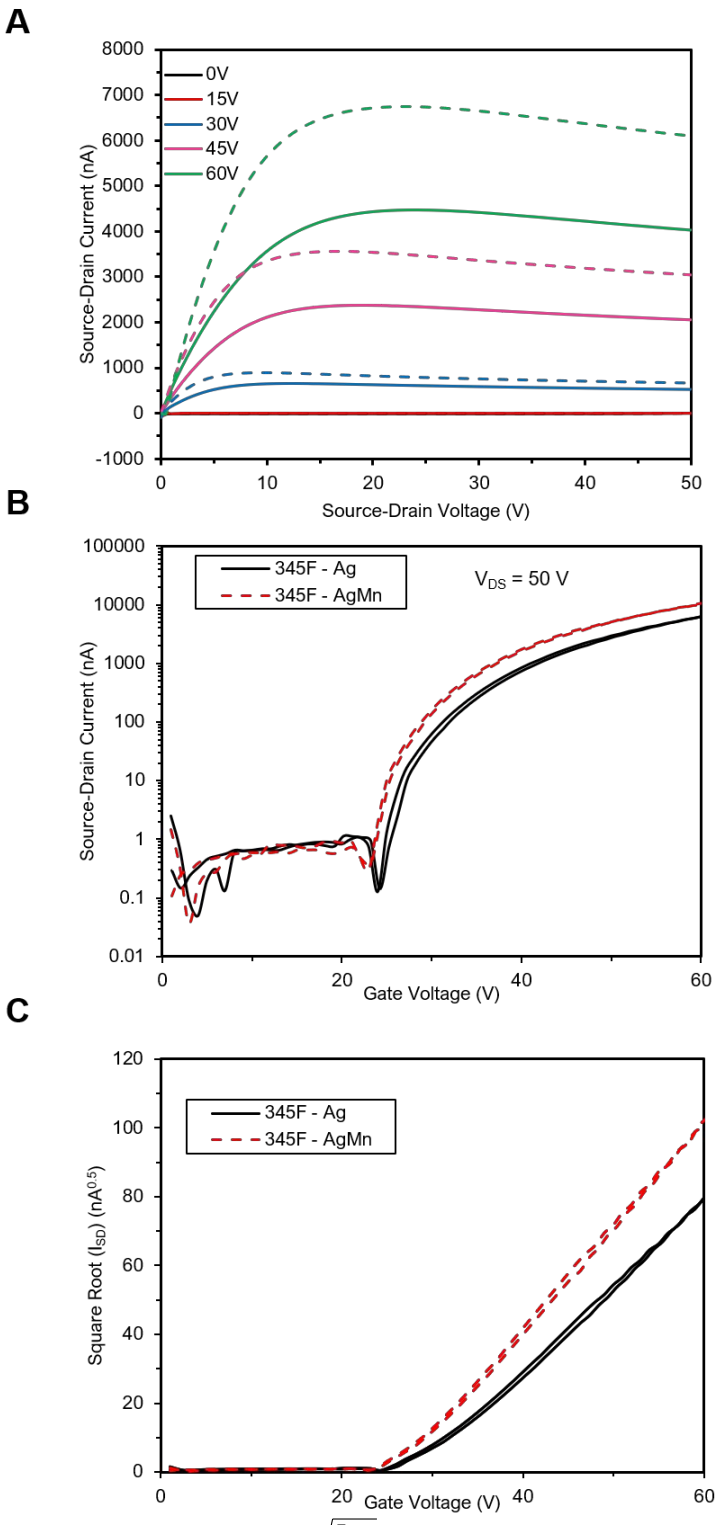

Figure S4: A A) Output, B) transfer and C) $\sqrt{I_{DS}}$ vs V_{GS} curves for 345F-SiPc (**2**) with Ag (solid lines) and Ag/Mn (dotted lines) electrode configurations.

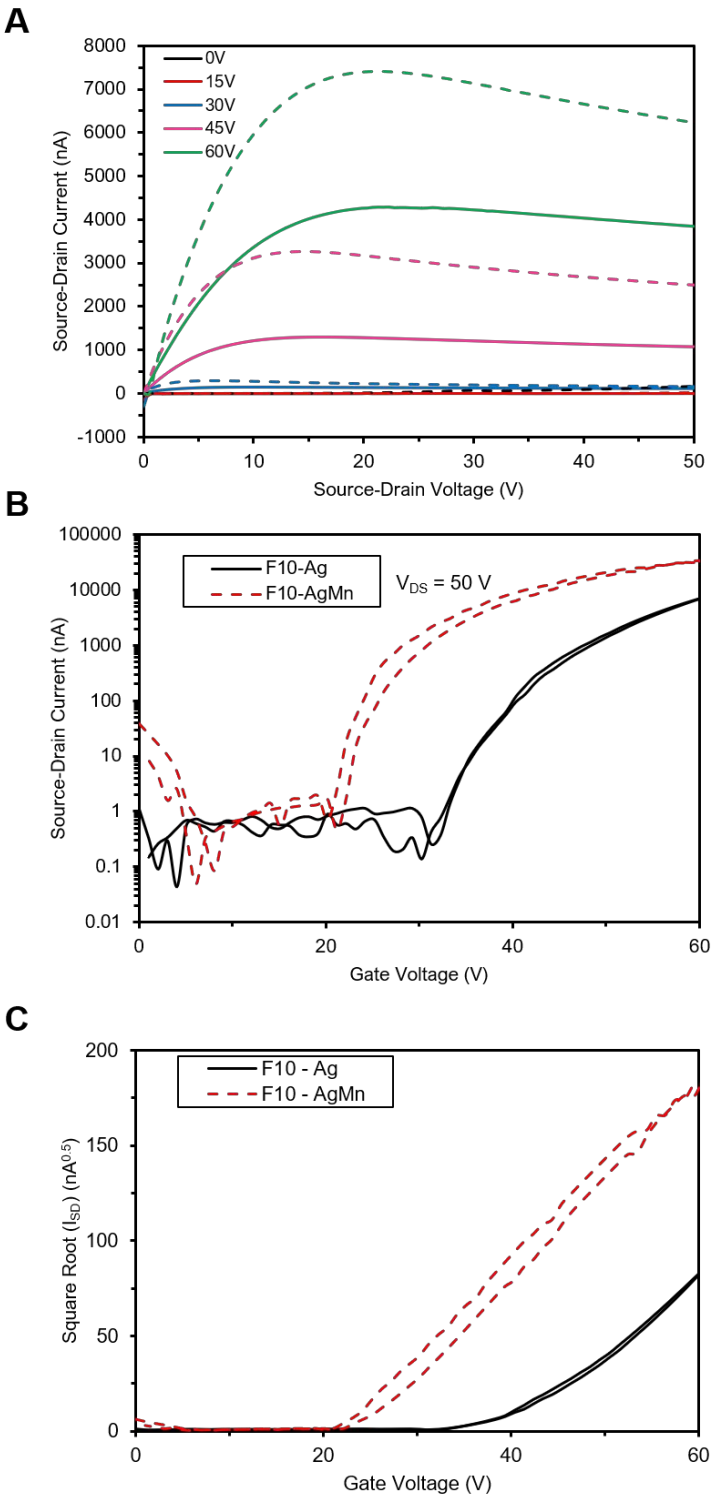

Figure S5. A) Output, B) transfer and C) $\sqrt{I_{DS}}$ vs V_{GS} curves for F_{10}-SiPc (3) with Ag (solid lines) and Ag/Mn (dotted lines) electrode configurations.

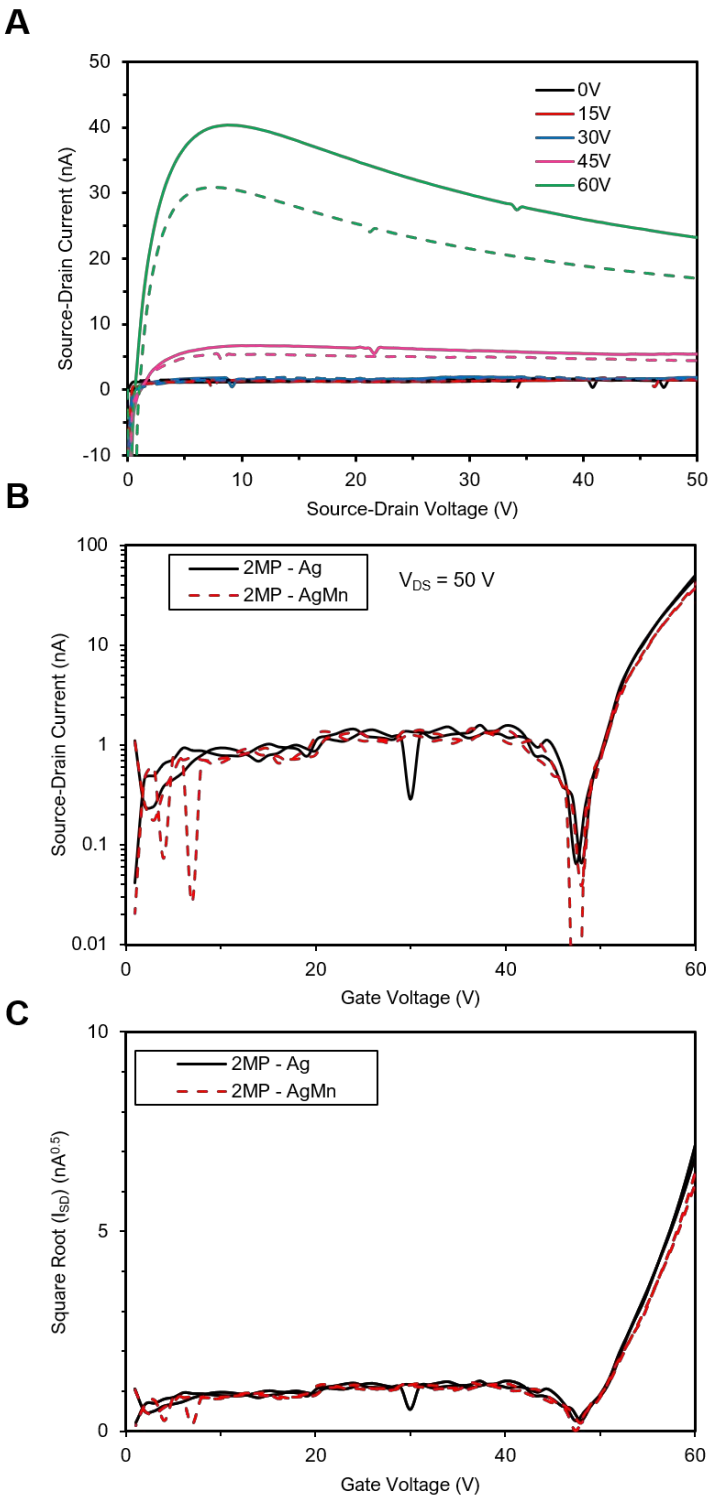

Figure S6: A) Output, B) transfer and C) $\sqrt{I_{DS}}$ vs V_{GS} curves for 2MP-SiPc (**4**) with Ag (solid lines) and Ag/Mn (dotted lines) electrode configurations.

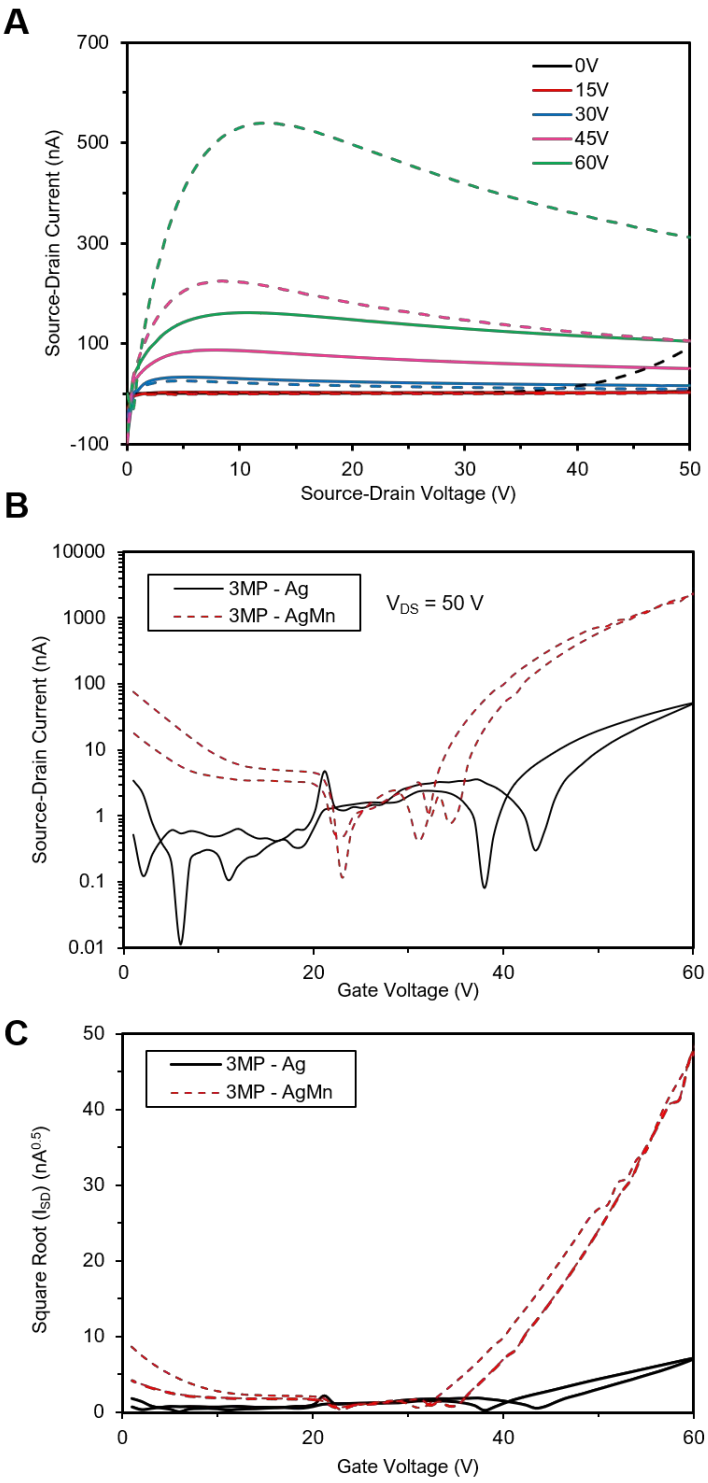

Figure S7: A) Output, B) transfer and C) $\sqrt{I_{DS}}$ vs V_{GS} curves for 3MP-SiPc (**5**) with Ag (solid lines) and Ag/Mn (dotted lines) electrode configurations.

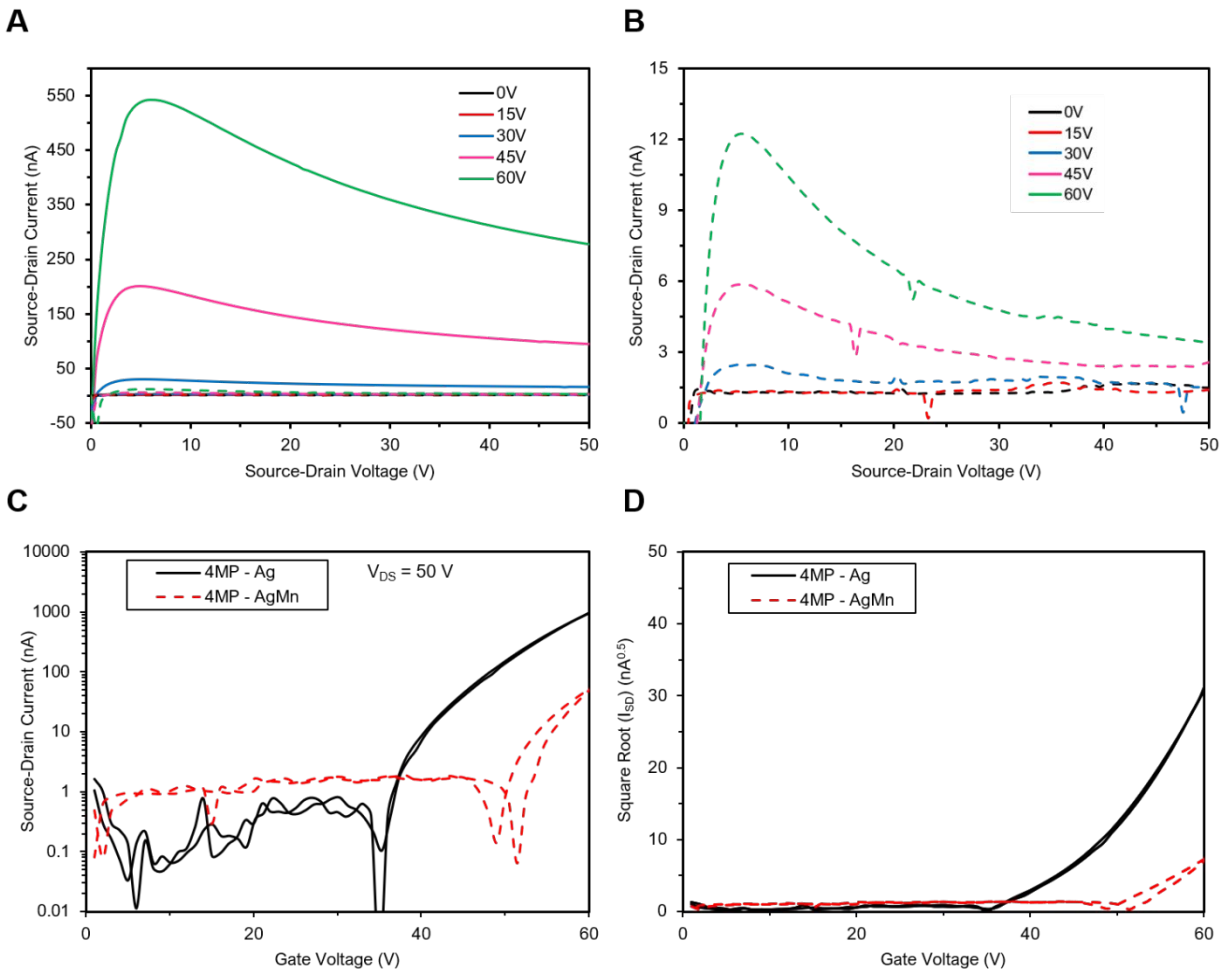

Figure S8: A and B) Output, C) transfer and D) $\sqrt{I_{DS}}$ vs V_{GS} curves for 4MP-SiPc (**6**) with Ag (solid lines) and Ag/Mn (dotted lines) electrode configurations.

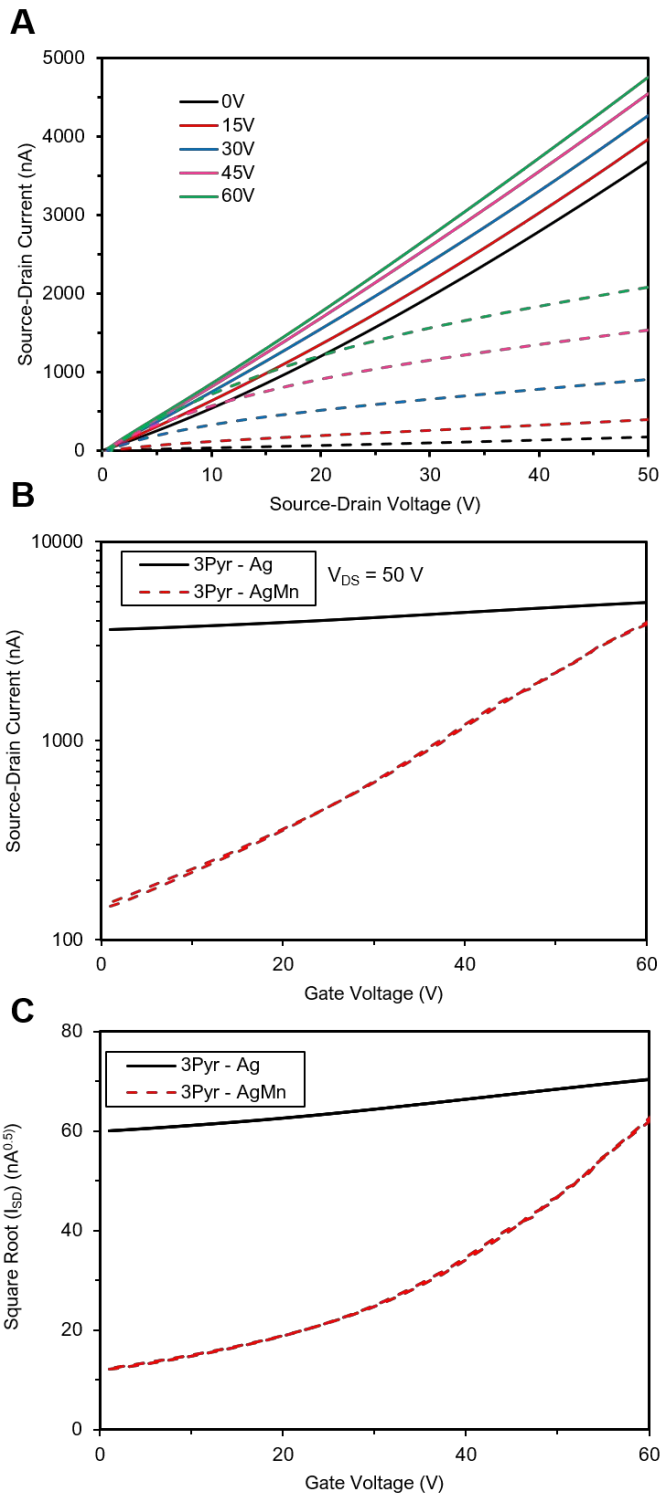

Figure S9: A) Output, B) transfer and C) $\sqrt{I_{DS}}$ vs V_{GS} curves for 3Pyr-SiPc (**7**) with Ag (solid lines) and Ag/Mn (dotted lines) electrode configurations.

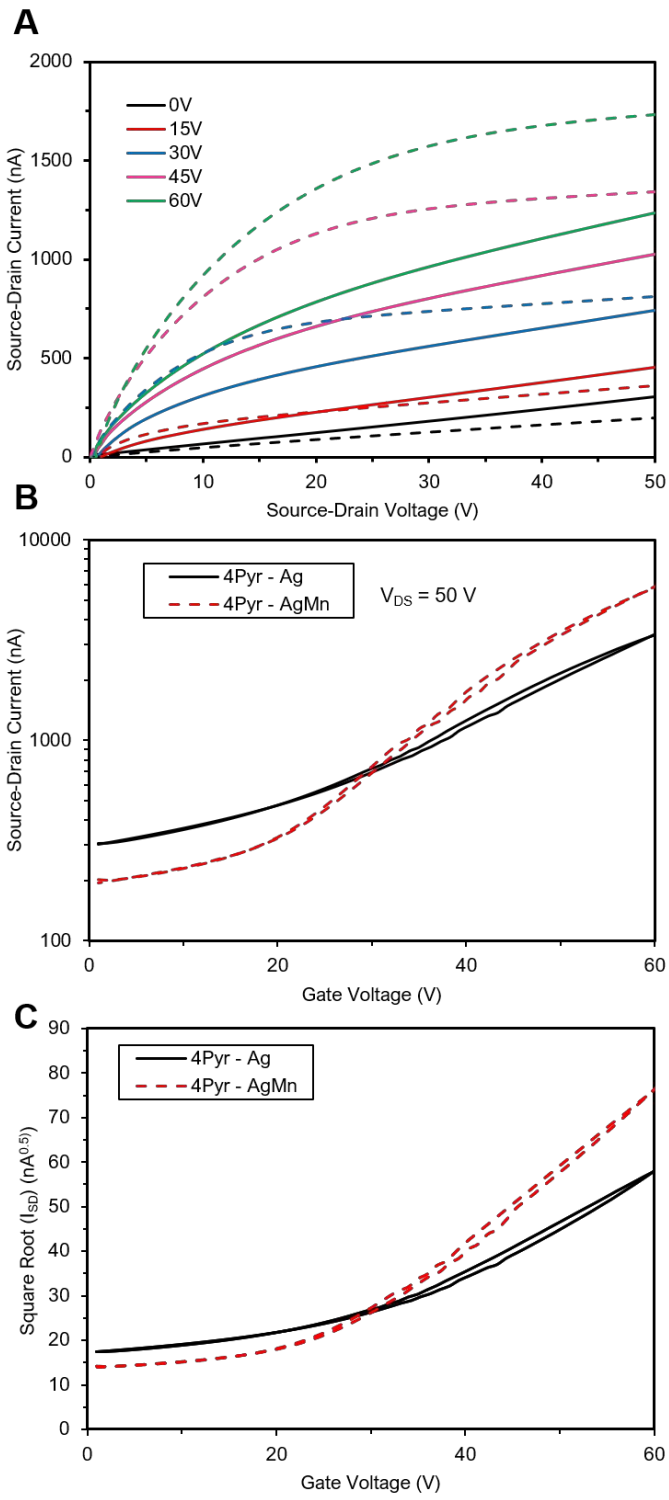

Figure S10: A) Output, B) transfer and C) $\sqrt{I_{DS}}$ vs V_{GS} curves for 4Pyr-SiPc (**8**) with Ag (solid lines) and Ag/Mn (dotted lines) electrode configurations.

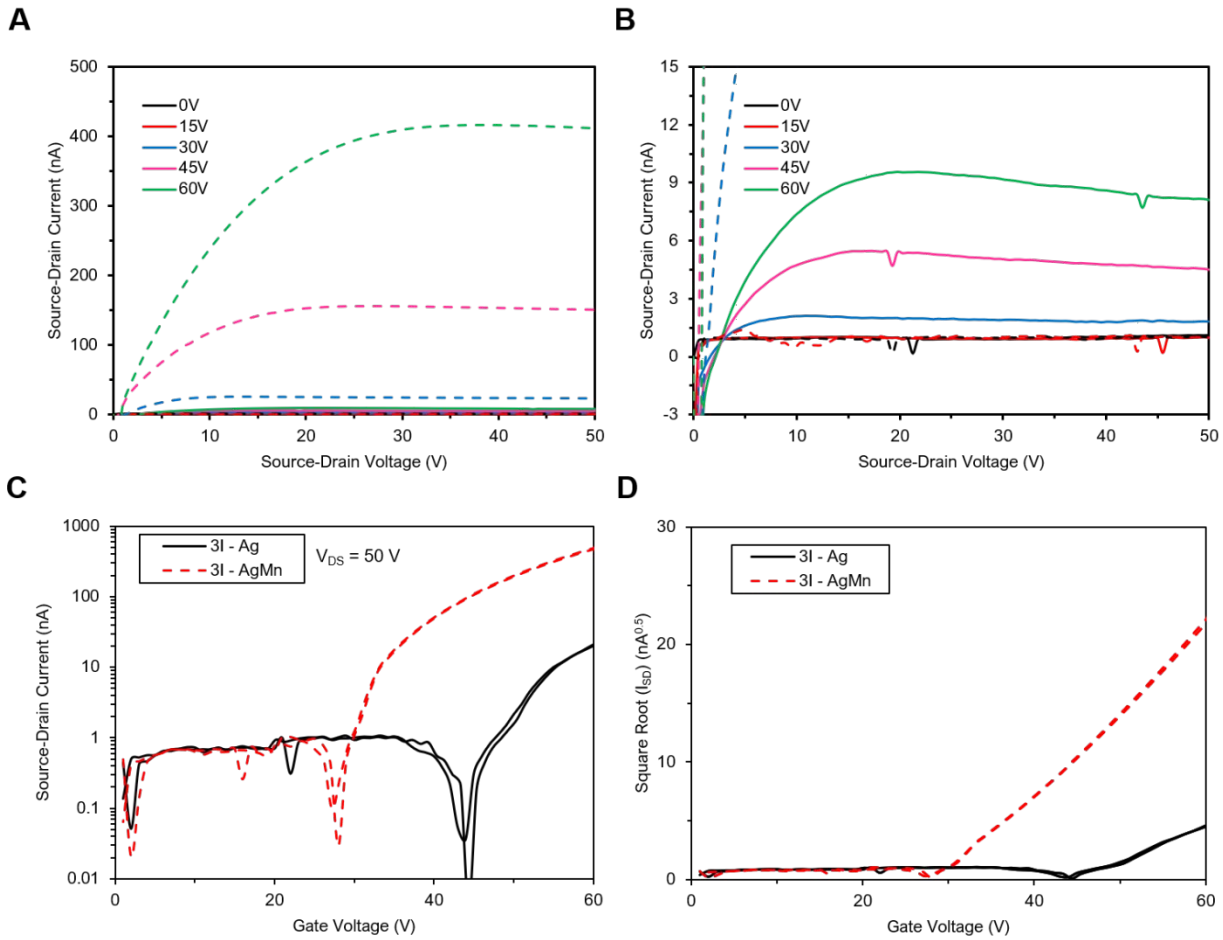

Figure S11: A and B) Output, C) transfer and D) $\sqrt{I_{DS}}$ vs V_{GS} curves for 3I-SiPc (**9**) with Ag (solid lines) and Ag/Mn (dotted lines) electrode configurations.

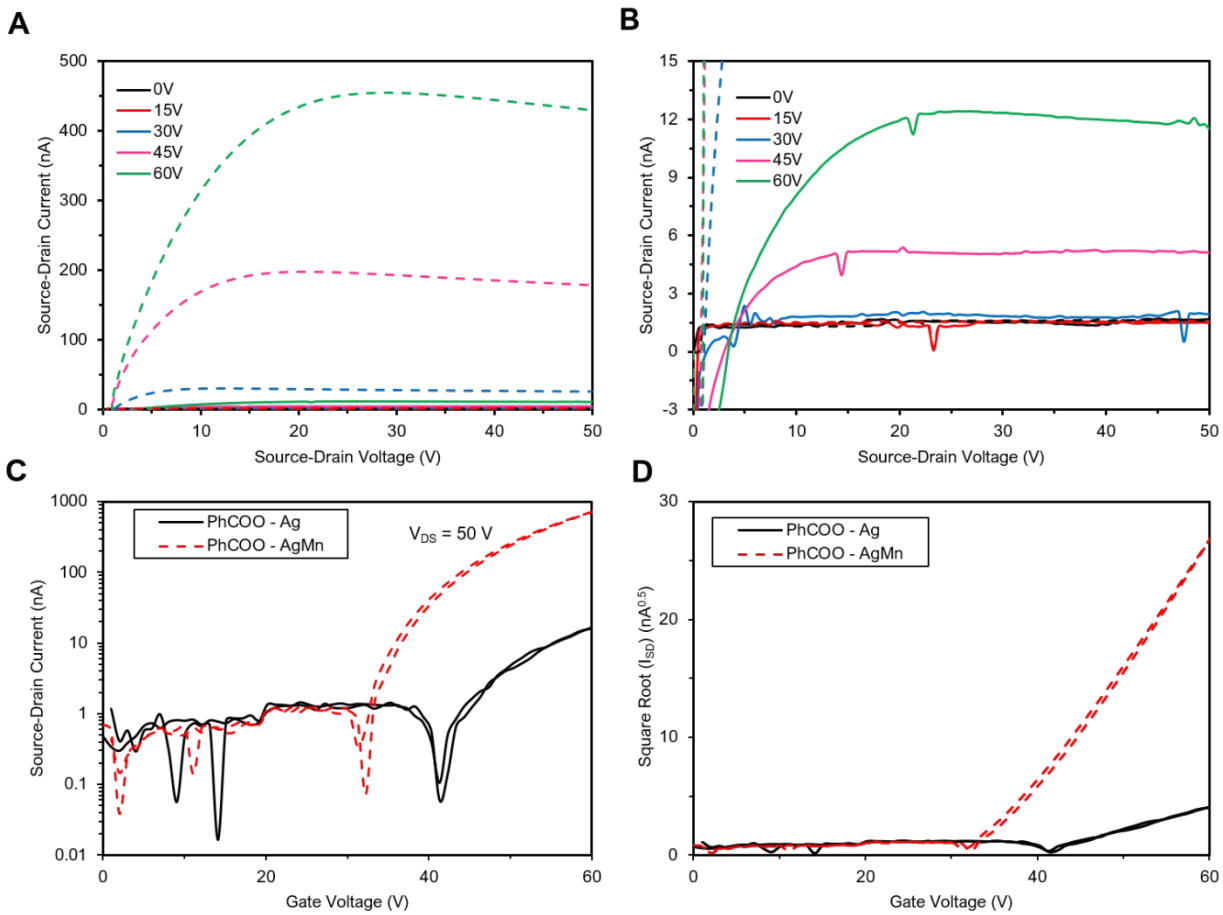

Figure S12: A and B) Output, C) transfer and D) $\sqrt{I_{DS}}$ vs V_{GS} curves for PhCOO-SiPc (**10**) with Ag (solid lines) and Ag/Mn (dotted lines) electrode configurations.

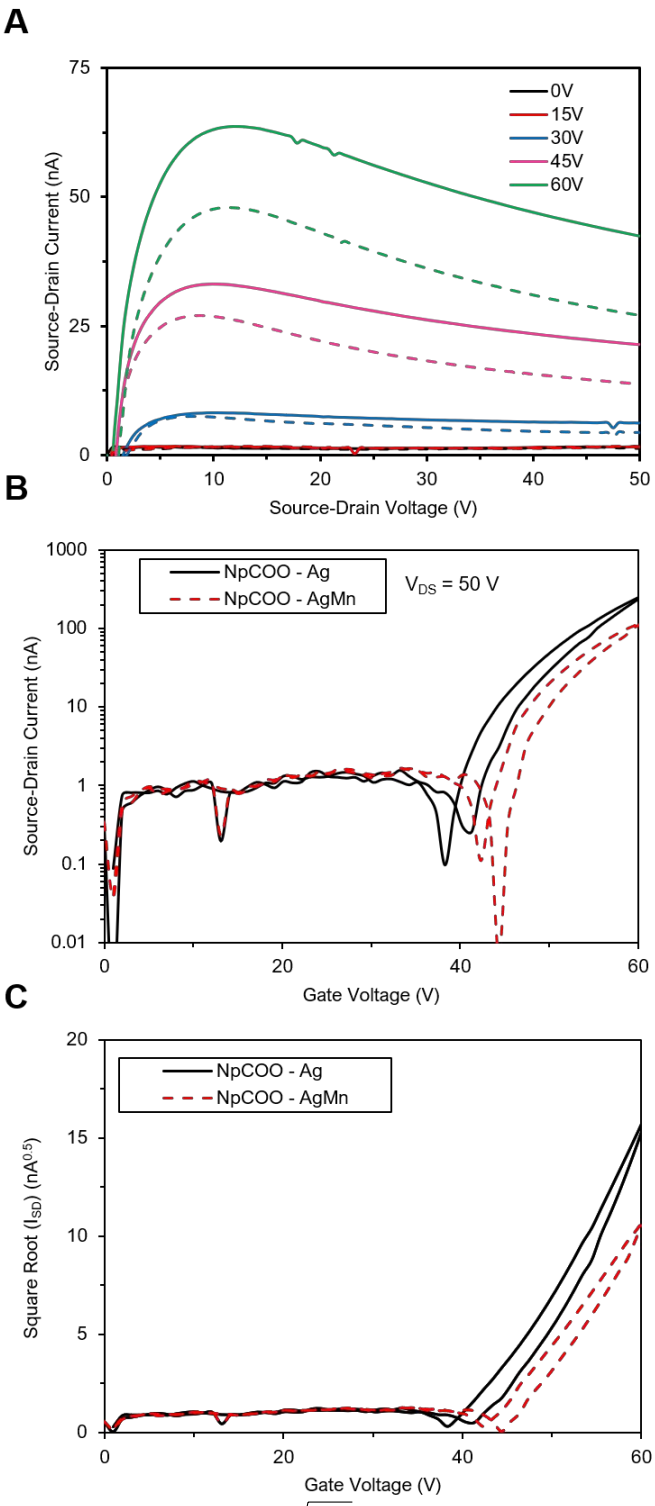

Figure S13: A) Output, B) transfer and C) $\sqrt{I_{DS}}$ vs V_{GS} curves for NpCOO-SiPc (**11**) with Ag (solid lines) and Ag/Mn (dotted lines) electrode configurations.

Additional PXRD and AFM Data

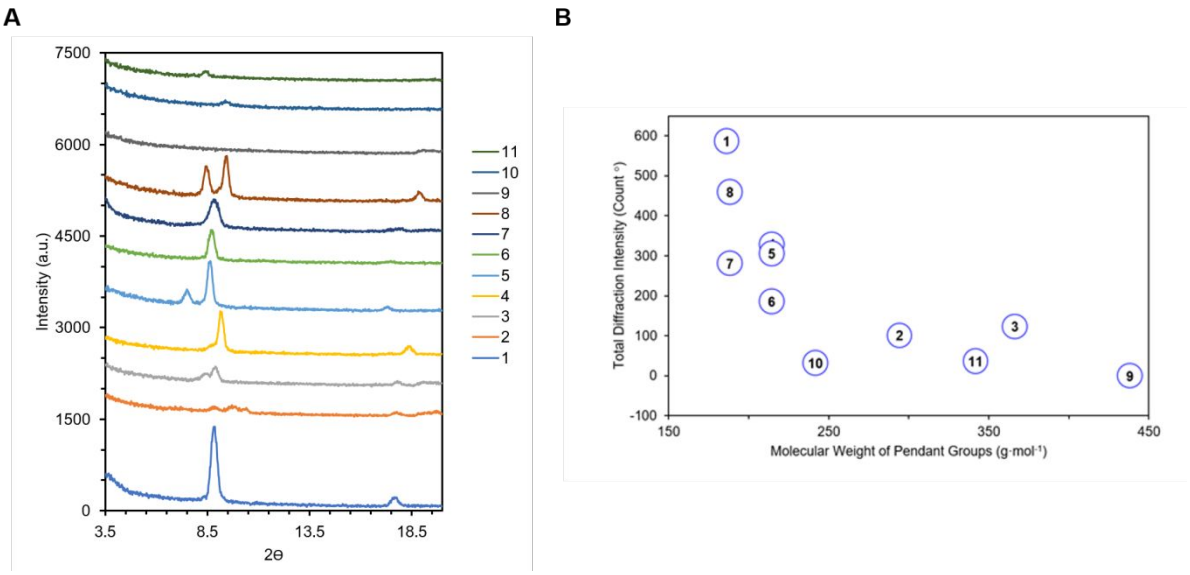

Figure S14. A) PXRD data for materials **1 – 11,** scanned from 3.5° < 2$\boldsymbol{\theta}$ < 20°, and B) total PXRD diffraction intensity for materials **1 – 11** as a function of pendant group molecular weight.

Table S4. Average RMS surface roughness of materials **1 – 11**, calculated from AFM images.

Material	Average RMS Roughness (nm)
1 (PhO-SiPc)	2.07
2 (345F-SiPc)	14.50
3 (F10-SiPc)	3.94
4 (2MP-SiPc)	2.70
5 (3MP-SiPc)	3.34
6 (4MP-SiPc)	2.33
7 (3Pyr-SiPc)	2.87
8 (4Pyr-SiPc)	2.05
9 (3I-SiPc)	9.11
10 (PhCOO-SiPc)	1.56
11 (NpCOO-SiPc)	2.58

Additional GIWAXS Data

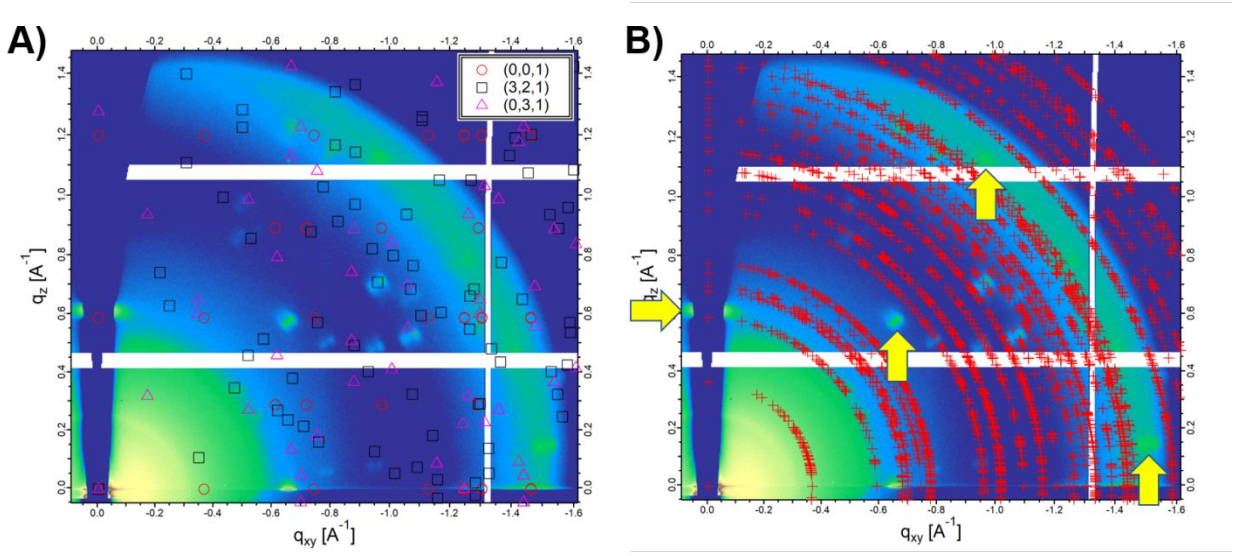

Figure S15. A) 2D scattering pattern with likely orientations based on simulated HKL orientations from -3 to +3 of the single crystal and B) reciprocal space map (RSM) model for all HKL orientations from -3 to +3 simulated, plotted over 2D scattering pattern and compared with magnitude of (q_{xy}, q_z) for material **1** (PhO-SiPc) at α = 0.2° determined by GIWAXS. Arrows indicate scattering data that does not correspond to single-crystal data.

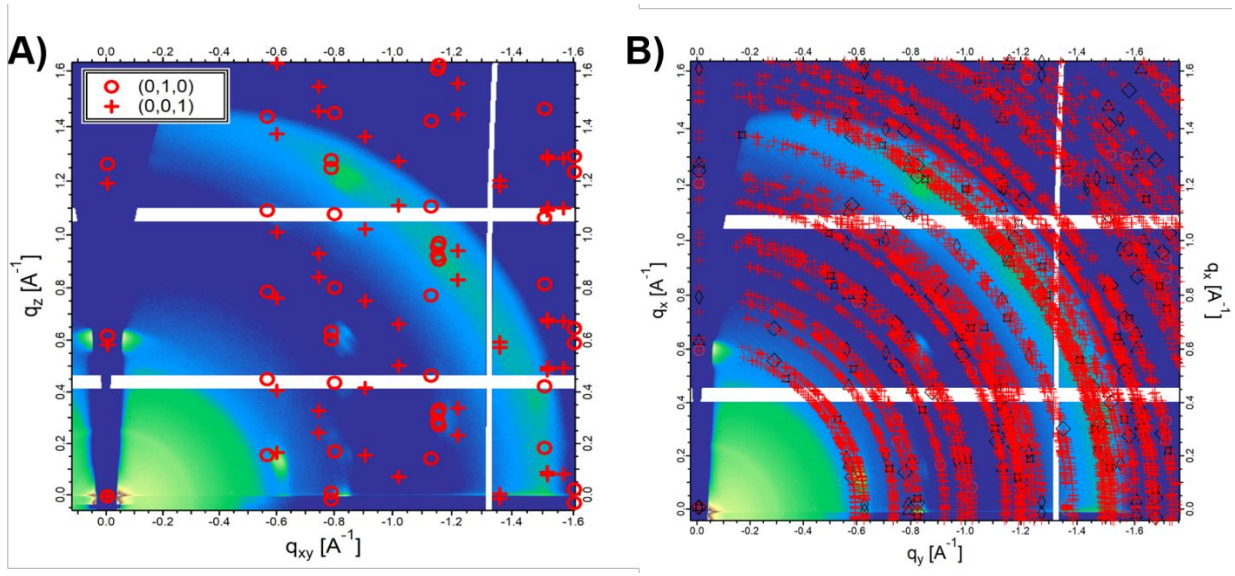

Figure S16. A) 2D scattering pattern with identified molecular orientations based on single crystal data and B) reciprocal space map (RSM) model for all HKL orientations from -3 to +3 simulated, plotted over 2D scattering pattern and compared with magnitude of (q_{xy}, q_z) for material **3** (F_{10}-SiPc) at α = 0.22° determined by GIWAXS.

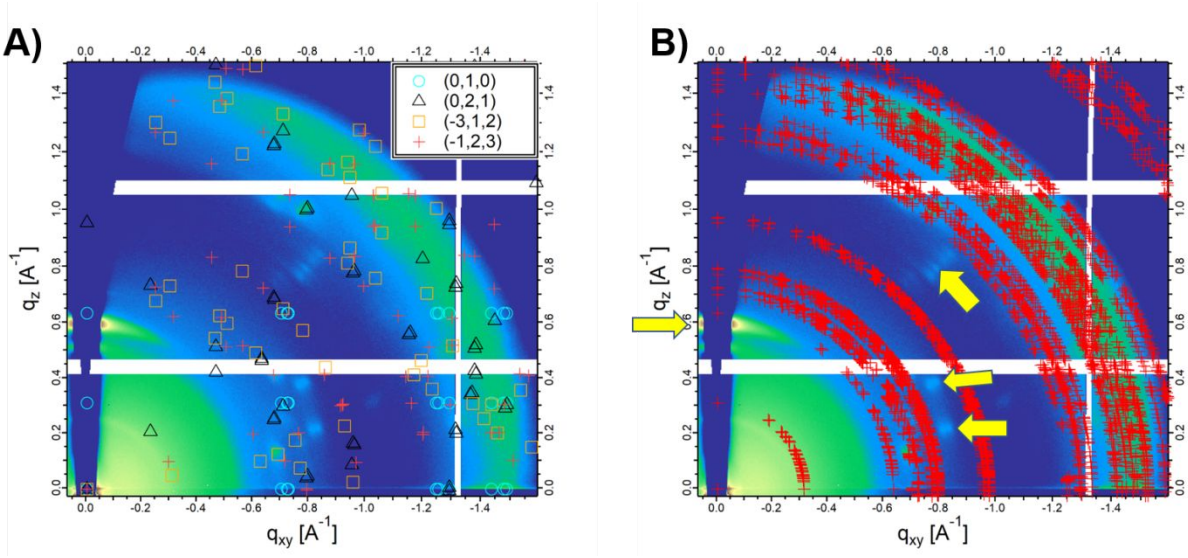

Figure S17. A) 2D scattering pattern with likely orientations based on simulated HKL orientations from -3 to +3 of the single crystal and B) reciprocal space map (RSM) model for all HKL orientations from -3 to +3 simulated, plotted over 2D scattering pattern and compared with magnitude of (q_{xy}, q_z) for material **5** (3MP-SiPc) at α = 0.2° determined by GIWAXS. Arrows indicate scattering data that does not correspond to single-crystal data.

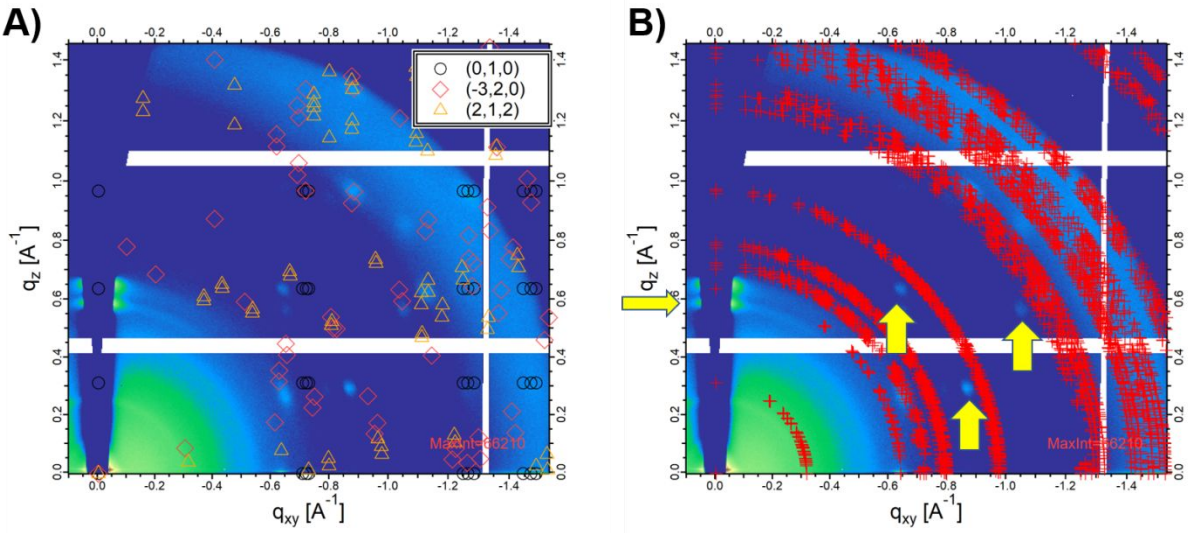

Figure S18. A) 2D scattering pattern with likely orientations based on simulated HKL orientations from -3 to +3 of the single crystal and B) reciprocal space map (RSM) model for all HKL orientations from -3 to +3 simulated, plotted over 2D scattering pattern and compared with magnitude of (q_{xy}, q_z) for material **8** (4Pyr-SiPc) at α = 0.22° determined by GIWAXS. Arrows indicate scattering data that does not correspond to single-crystal data.

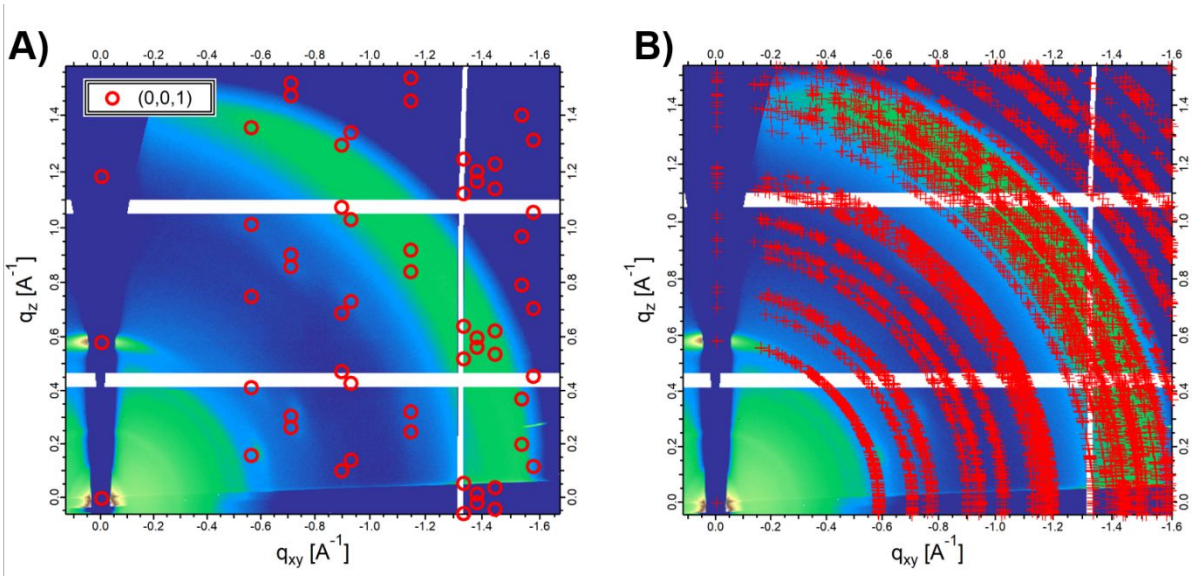

Figure S19. A) 2D scattering pattern with identified molecular orientations based on single crystal data and B) reciprocal space map (RSM) model for all HKL orientations from -3 to +3 simulated, plotted over 2D scattering pattern and compared with magnitude of (q_{xy}, q_z) for material **11** (NpCOO-SiPc) at α = 0.22° determined by GIWAXS**.**

Solid State UV-Vis Data

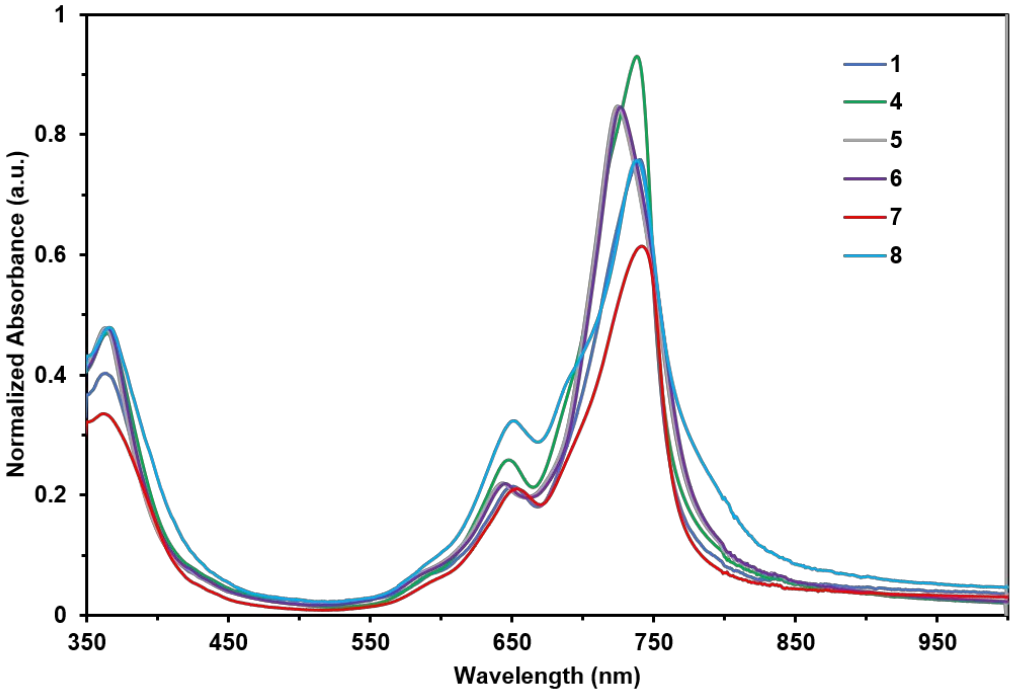

Figure S20: Solid state UV-Vis spectra for previously unreported SiPcs in OTFTs.